

Short thesis for the degree of doctor of philosophy (PhD)

**Oxidation of ammonia and amino acids by
hypochlorous acid: kinetics and mechanism**

by Fruzsina Simon

Supervisor: Dr. István Fábíán



UNIVERSITY OF DEBRECEN

Doctoral School of Chemistry

Debrecen, 2023.

Introduction and objectives

Nowadays the reactions between hypochlorous acid and amino compounds are still thoroughly studied due to its importance in environmental chemistry and *in vivo* processes. These reactions yield chloramines which have different compositions depending on the actual conditions. Depending on the pH and the concentration of HOCl, they can form mono- and dichlorinated amino compounds, and in the case of ammonia also trichloramine.

The formation of *N*-chlorinated compounds is important in several areas. Chlorine and hypochlorous acid are mostly used as disinfectants in wastewater and drinking water treatment technologies. Thus, the chloramines can easily be formed from ammonia, amino compounds and amino acids in the treated water. They are considered as secondary disinfectants, because they are able to kill microorganisms and viruses, although with less efficiency than chlorine or hypochlorous acid. However, they also have a negative effect due to their significant contribution to the formation of toxic disinfection by-products (DBPs). Accordingly, the chemistry of these compounds is of relevance in environmental chemistry.

Similar processes also occur and lead to the formation of *N*-chloramines in living organisms. The process of inflammation is the body's natural defense mechanism. The myeloperoxidase enzyme is a so-called inflammatory mediator molecule that produces hypochlorous acid from chloride ion and hydrogen peroxide. HOCl is a relatively stable compound with a strong anti-pathogenic effect, it accumulates in the body during diseases and reacts with various biologically significant molecules, such as amino acids, peptides and proteins.

It is well known that chloramines are unstable, and depending on their composition they are precursors of the formation of many molecules that may have toxic effects in the living organism.

The reactions and biological impacts of *N*-chloramines and *N*-chloroamino acids have extensively been studied before. Despite this, most of the data are contradictory, and no or very limited number of reliable data can be found on the formation and decomposition processes of *N,N*-dichloroamino acids. In order to obtain more information about the properties of the mentioned compounds, detailed studies are required on their reactions. These studies should focus on the formation and identification of the reactive intermediates and the competing reaction paths yielding the final products.

The aim of our work is to investigate the formation and decomposition kinetics of selected *N*-chlorinated compounds, to develop detailed mechanisms for the overall processes and to resolve the discrepancies found in the relevant literature.

Instrumentation and computational methods

Redox and pH-potentiometric titrations were performed with a Metrohm 888 Titrand automatic titrator, to which a combined platinum electrode Metrohm 6.0451.100 and a combined glass electrode Metrohm 6.0262.100 were connected. For pH measurements we used a Metrohm 6.0234.100 microelectrode connected to a Metrohm 913 pH meter. The electrodes were calibrated daily using potassium hydrogen phthalate (0.05 M) and borax (0.01 M) standard solutions. The data obtained during the pH readings were converted as reported by Irving et al., and $\text{pH} = -\log[\text{H}^+]$ in the thesis.

The acid dissociation constants of the amino acids were determined by pH metric titration, and the experimental data were evaluated using the SUPERQUAD software.

An Applied Photophysics SX-20 type *stopped-flow* device was used for monitoring the formation of the *N*-chloro compounds. The detector was a photoelectron multiplier. A single kinetic curve was obtained as the average of 3 to 5 replicate kinetic runs. The Spectra Kinetics function of the software was used to record several kinetic curves simultaneously. The OriginPro 2018 program was used to fit the kinetic curves using the appropriate functions and a non-linear least squares routine.

An Agilent Technologies Cary 8454 UV – Vis diode array spectrophotometer was used to monitor the decomposition reactions. The temperature of the measuring cell was kept constant with built-in Peltier type thermostat. In most cases the spectral changes were followed in the 200 - 400 nm wavelength range.

NMR measurements were performed using a Bruker DRX 400 (9.4 T) spectrometer. The spectrometer equipped with a Bruker VT-1000 temperature controller and a BB inverted gradient head (5 mm). We used a water suppression technique during the experiments, since we worked with aqueous solutions. Proton signals in water (4.8 ppm) were eliminated with a watergate pulse sequence (12.6 dB). DSS was used as an external standard to determine the chemical shift of the ^1H NMR signals. The ^1H NMR spectra were acquired by 32 scans with an acquisition time of 1.366 s. The spectra were analyzed with Bruker WinNMR and MestReNova software packages.

Ion chromatography (IC) experiments were performed with a Thermo 5000+ two-channel ion chromatograph. The anionic exchange columns were Dionex IonPacTMAG14 and Dionex IonPacTMAS14.

New scientific results

1. In the ammonia - hypochlorous acid system, the formation kinetics of mono-, di- and trichloramine was studied in detail under acidic conditions. The rate equations for each reaction step and the corresponding rate constants were determined.

1.1. The direct reaction between ammonium ion and hypochlorous acid is relatively slow, a first-order process for both reactants, in which only the formation of trichloramine can be observed even at a significant excess of NH_4^+ .

In the NH_4^+ - HOCl reaction, the spectral changes at the absorbance maxima (220 and 336 nm) can clearly be assigned to the formation of NCl_3 (Figure 1). We verified that NH_2Cl and $NHCl_2$ do not even temporarily accumulate in the reaction system.

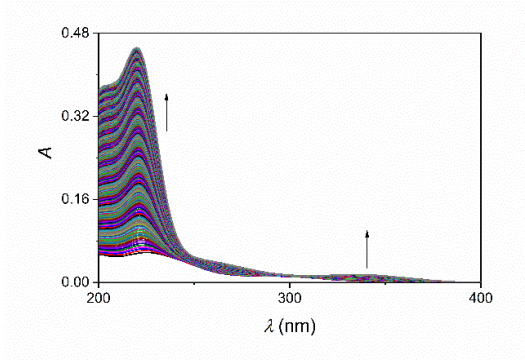
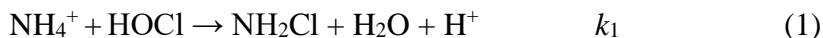


Figure 1. Time resolved spectral changes during reaction of NH_4^+ and HOCl.

$c_{NH_3}^0 = 2.50 \times 10^{-3}$ M, $c_{HOCl}^0 = 2.50 \times 10^{-3}$ M, pH = 1.95, $I = 1.00$ M (NaClO₄), $T = 25.0$ °C, $\Delta t = 29$ s, $t = 7200$ s.

Based on the method of initial rates, we verified that the rate-determining step of the process is first-order for both NH_4^+ and HOCl , i.e. overall, it is a second-order process.

The experimental results can be interpreted by considering that monochloramine forms in a relatively slow rate-determining step (1) and is oxidized to trichloramine in fast subsequent reaction steps (vide infra).



The rate constant (k_1) was estimated by fitting the kinetic curves recorded at a wavelength of 220 nm (Table 1).

1.2. We have confirmed that the relatively fast oxidation of monochloramine by hypochlorous acid is an overall second-order – first-order for both reactants – process, and that the pH dependence of the rate constant can be interpreted by the protonation reaction of monochloramine. The rate of acid-catalyzed decomposition and oxidation of monochloramine is comparable when the concentration ratio of HOCl : NH₂Cl is less than 0.7 : 1.0.

NH_2Cl was prepared in a slightly alkaline medium and reacted with one equivalent HOCl in an acidic medium. Under these conditions, the spectral changes are consistent with the conversion of monochloramine to dichloramine (Figure 2).

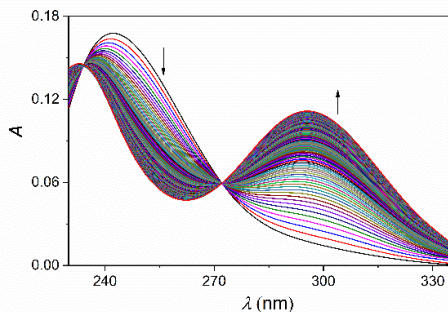


Figure 2. Time resolved spectral changes during the oxidation of NH_2Cl to NHCl_2 . (NH_2Cl : $\lambda_{\text{max}} = 243$ nm, NHCl_2 : $\lambda_{\text{max}} = 292$ nm).

$c_{\text{NH}_2\text{Cl}}^0 = 5.00 \times 10^{-4}$ M, $c_{\text{HOCl}}^0 = 5.00 \times 10^{-4}$ M, pH = 1.92, $I = 1.00$ M (NaClO_4), $T = 25.0$ °C, $t = 7$ s.

The kinetic curves can be interpreted by considering reactions (2) and (3) (Figure 3).

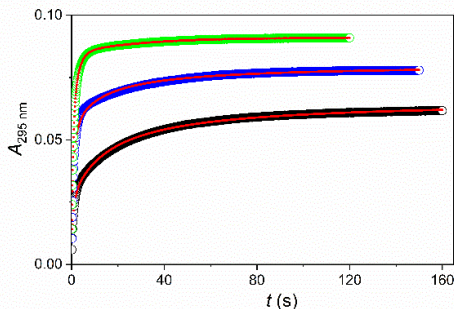
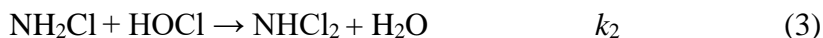
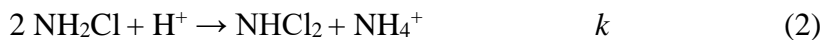


Figure 3. Kinetic traces in the reaction of NH_2Cl with HOCl . Experimental (markers) and fitted kinetic traces on the basis of eq.s 2 and 3 (solid lines). $c_{\text{NH}_2\text{Cl}}^0 = 5.00 \times 10^{-4}$ M, $c_{\text{HOCl}}^0 = \bullet 1.00 \times 10^{-4}$ M, $\bullet 2.00 \times 10^{-4}$ M, $\bullet 3.00 \times 10^{-4}$ M, pH = 1.92, $I = 1.00$ M (NaClO_4), $T = 25.0$ °C.

When greater than 0.8 equivalent HOCl is reacted with NH₂Cl, the kinetic curves can be fitted by considering only reaction (3). The rate constants of equations (2) and (3) show a clear pH dependence which is interpreted by the protonation equilibrium of NH₂Cl (4).



$$K_p = \frac{[\text{NH}_3\text{Cl}^+]}{[\text{NH}_2\text{Cl}] [\text{H}^+]}$$

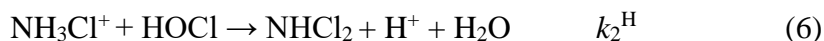
It was previously established that the decomposition of monochloramine occurs via the reaction between monochloramine and its protonated forms (5).



i. e.

$$k = k^H \times \frac{K_p[\text{H}^+]}{1 + K_p[\text{H}^+]}$$

We have shown that the acidic form of monochloramine is reactive in the oxidation by hypochlorous acid (Figure 4).



i. e.

$$k_2 = k_2^H \times \frac{K_p[\text{H}^+]}{1 + K_p[\text{H}^+]}$$

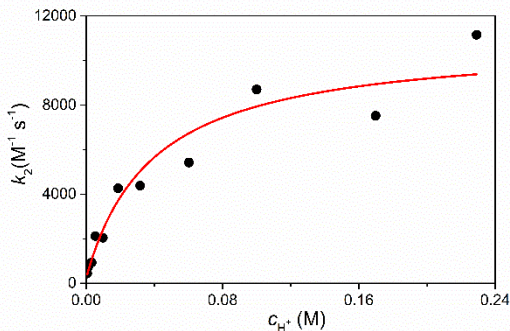


Figure 4. pH dependence of k_2 as a function of H^+ concentration. $c_{NH_2Cl}^0 = 5.00 \times 10^{-4}$ M, $c_{HOCl}^0 = 5.00 \times 10^{-4}$ M, $I = 1.00$ M ($NaClO_4$), $T = 25.0$ °C.

1.3. We have shown that the oxidation of dichloramine to trichloramine is first-order with respect to $NHCl_2$ and second-order with respect to $HOCl$, i.e. a third-order process overall. The results are interpreted by considering that Cl_2O always forms from $HOCl$ in a rapid pre-equilibrium in the reaction system, and it oxidizes $NHCl_2$ significantly faster than $HOCl$. We have shown that dichlorine monoxide is not involved in the oxidation of monochloramine.

A stable $NHCl_2$ solution could not be produced by oxidizing monochloramine with one equivalent hypochlorous acid, so the formation of NCl_3 was studied by oxidizing NH_2Cl with 1.5 – 15 equivalents of $HOCl$. The reaction shows complex kinetic pattern; the first fast and the second, relatively slow sections of the kinetic curves are assigned to the formation of $NHCl_2$ (3) and NCl_3 (7), respectively (Figure 5).

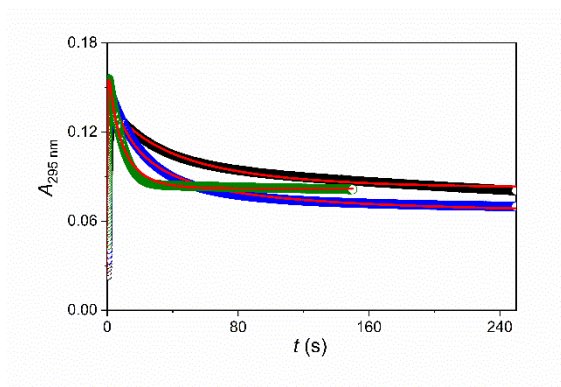


Figure 5. Kinetic traces of NCl_3 formation. Experimental (markers) and fitted kinetic curves on the basis of eq.s (3) and (7) (solid lines).

$c_{\text{NH}_2\text{Cl}}^0 = 5.00 \times 10^{-4} \text{ M}$, $c_{\text{HOCl}}^0 = \bullet 7.50 \times 10^{-4} \text{ M}$, $\bullet 1.00 \times 10^{-3} \text{ M}$, $\bullet 1.50 \times 10^{-3} \text{ M}$, $I = 1.00 \text{ M}$ (NaClO_4), $T = 25.0 \text{ }^\circ\text{C}$.

The kinetic curves were fitted taking into account reactions (3) and (7), assuming that both reaction steps are first order for HOCl and the given chloramine.



The values obtained for rate constant k_2 are in good agreement with the results detailed above. We proved that k_2 is independent of the concentration of HOCl.

We have shown that k_3 linearly depends on the HOCl concentration (Figure 6), i.e. reaction (7) is second-order for HOCl. This confirms that Cl_2O , being in fast preequilibrium with HOCl, is the reactive species in the oxidation of NHCl_2 .

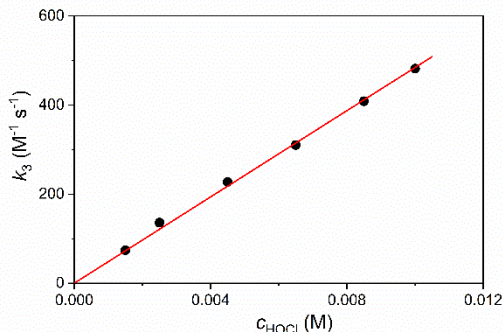


Figure 6. The second order rate constants of the NCl_3 formation as a function of HOCl concentration.

$c_{\text{NH}_2\text{Cl}}^0 = 5.00 \times 10^{-4} \text{ M}$, $I = 1.00 \text{ M}$ (NaClO_4), $T = 25.0 \text{ }^\circ\text{C}$.



$$K_1 = \frac{[\text{Cl}_2\text{O}]}{[\text{HOCl}]^2}$$



i. e.

$$k_3 = k_{\text{Cl}_2\text{O}} K_1 [\text{HOCl}]$$

We have confirmed that the $k_{\text{Cl}_2\text{O}}K_1$ coefficient shows definite pH dependence in the 0.7 - 3.2 pH region. This is a strong indication that dichloramine is also involved in an acid-base equilibrium, and its acidic form, NH_2Cl_2^+ , is reactive in reaction (9).

Table 1. summarizes the individual reaction steps in the ammonium ion – hypochlorous system and the corresponding rate constants.

Table 1. The reactions in the $\text{NH}_4^+ + \text{HOCl}$ system and their rate constants.

Reaction	Parameter	
$\text{NH}_2\text{Cl} + \text{H}^+ \rightleftharpoons \text{NH}_3\text{Cl}^+$	$K_p^{a, b}$	4.35×10^1
$\text{NH}_2\text{Cl} + \text{NH}_3\text{Cl}^+ \rightarrow \text{NHCl}_2 + \text{NH}_4^+$	$k^{H a, c}$	3.35×10^2
$\text{NH}_4^+ + \text{HOCl} \rightarrow \text{NH}_2\text{Cl} + \text{H}_2\text{O} + \text{H}^+$	k_1^c	$(2.0 \pm 0.6) \times 10^{-1}$
$\text{NH}_3\text{Cl}^+ + \text{HOCl} \rightarrow \text{NHCl}_2 + \text{H}_2\text{O} + \text{H}^+$	$k_2^{H c}$	$(9.6 \pm 0.6) \times 10^3$
$2 \text{HOCl} \rightleftharpoons \text{Cl}_2\text{O} + \text{H}_2\text{O}$	K_1^b	1.15×10^{-2}
$\text{NHCl}_2 + \text{Cl}_2\text{O} \rightarrow \text{NCl}_3 + \text{HOCl}$	$k_{\text{Cl}_2\text{O}} K_1^{d, e}$	$(1.58 \pm 0.01) \times 10^3$

a: P. Fehér et al. (2019) Dalton Trans., 48(44), 16713–16721., b: M^{-1} ,
c: $\text{M}^{-1} \text{s}^{-1}$, d: $\text{M}^{-2} \text{s}^{-1}$, e: at pH = 1.00.

2. We have studied the formation kinetics of *N*-methyl-*N*-monochloro derivatives in the reactions between five *N*-methylamino acids and hypochlorous acid in detail. It was confirmed that these are second-order processes, i.e. first-order for both the amino acid and HOCl. The pH dependence of the rate constants is explained by the protolytic equilibria of the reactants. We have confirmed that the activated complexes in these reactions are characterized by stronger bonds and less organized structures compared to the corresponding chlorination reactions of unsubstituted amino acids.

The formation of *N*-chloro-*N*-methylamino acids from *N*-methylamino acids and hypochlorous acid occurs according to the following second-order rate equation:

$$\frac{dc_{NCAA}}{dt} = k_{\text{obs}}^{2\text{nd}} c_{\text{HOCl}} c_{\text{AA}} \quad (10)$$

where c_{HOCl} and c_{AA} are the total concentrations of hypochlorous acid and *N*-methylamino acid, respectively.

The characteristic bell-shaped pH dependence of the rate coefficients, $k_{\text{obs}}^{2\text{nd}}$, proves that the reaction takes place between HOCl and the fully deprotonated form of the amino acid ($\text{CH}_3\text{NH-CH(R)-COO}^-$) (11) (Figure 7).



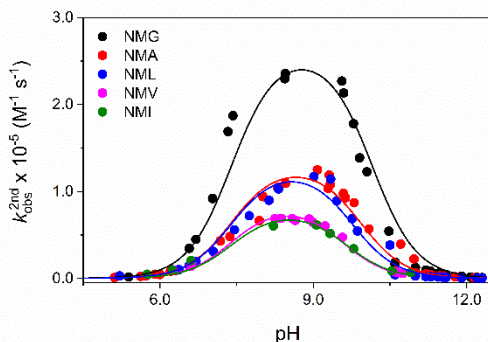


Figure 7. The pH dependence of $k_{\text{obs}}^{2\text{nd}}$. Experimental data (markers) and fitted curves according to (12) (solid lines).

$c_{\text{AA}}^0 = 7.50 \times 10^{-4} \text{ M}$, $c_{\text{HOCl}}^0 = 5.00 \times 10^{-4} \text{ M}$, $I = 1.00 \text{ M}$ (NaClO_4), $T = 25.0 \text{ }^\circ\text{C}$.

The pH-dependent second-order rate constants were fitted to equation (12) and the pH-independent second-order rate coefficient (k) was determined (Table 2).

$$k_{\text{obs}}^{2\text{nd}} = k \frac{K_{\text{AA}}[\text{H}^+]}{(K_{\text{AA}} + [\text{H}^+])(K_{\text{HOCl}} + [\text{H}^+])} \quad (12)$$

where K_{AA} and K_{HOCl} are the acid dissociation constants of the amino acid and hypochlorous acid, respectively.

Similarly to the *N*-chlorination reactions of protein-forming amino acids, the value of the rate coefficients is $\sim 10^7 \text{ M}^{-1} \text{ s}^{-1}$. In the case of *N*-methylglycine, the *N*-methyl group significantly increases the basicity of the amino group compared to the other *N*-methylated amino acids, thereby it becomes more active in a reaction with an electrophilic reactant. In the case of amino acids containing an alkyl group on the α -carbon atom, this effect is smaller due to the electron-donating α -substituent. In the case of amino acids with branched alkyl side chains, the relatively large side chain and the *N*-methyl substituent together

sterically inhibit the attack of hypochlorous acid that leads to a decrease in reactivity.

Table 2. Kinetic parameters for the *N*-chlorination of *N*-methyl amino acids and the corresponding α -amino acids.

$I = 1.00 \text{ M (NaClO}_4\text{)}, T = 25.0 \text{ }^\circ\text{C}.$

Amino acid	$k \times 10^{-7}$ ($\text{M}^{-1} \text{s}^{-1}$)	ΔS^\ddagger ^c ($\text{J mol}^{-1} \text{K}^{-1}$)	ΔH^\ddagger ^d (kJ mol^{-1})	pK_{AA}
<i>N</i> -methylglycine	14.7 ± 0.4	-29.9 ± 1.0	18.8 ± 0.3	10.15 ± 0.01
glycine ^a	3.94	-36.8	18.1	9.42
<i>N</i> -methylalanine	4.29 ± 0.09	-33.3 ± 6.3	19.0 ± 2.0	9.92 ± 0.01
α -alanine ^a	2.91	-37.1	18.4	9.60
<i>N</i> -methylleucine	2.89 ± 0.07	3.7 ± 1.7	31.2 ± 0.5	9.76 ± 0.01
leucine ^a	2.90	-73.1	7.73	9.49
<i>N</i> -methylisoleucine	1.38 ± 0.06	-10.1 ± 2.8	27.8 ± 0.9	9.65 ± 0.05
isoleucine ^a	2.65	-59.0	12.3	9.46
<i>N</i> -methylvaline	1.24 ± 0.02	-17.0 ± 2.8	26.1 ± 0.9	9.57 ± 0.01
valine ^a	3.35	-60.0	12.1	9.41

a: M. Szabó, F. Simon, I. Fábíán., *Wat. Res.*, **2019**, 165, 114994.

We have determined the activation parameters for the formation of *N*-chloro-*N*-methylamino acids (eq. 11) and compared them to the data obtained for amino acids without a methyl group on the nitrogen atom (Table 2). Overall, it is concluded that a stronger bond is formed

between the reactants, but the structure becomes less organized in the activated complex in the reactions of *N*-methylated branched chain amino acids. This phenomenon is the result of the positive inductive effect of the alkyl side chain and the *N*-methyl group induced by HOCl and steric effects.

3. We have shown that the *N*-chloro-*N*-methylamino acids decompose more than one order of magnitude faster than *N*-chlorinated amino acids without a methyl substituent. We have confirmed that the decomposition reactions are first-order for *N*-chloro-*N*-methylamino acids, their reaction rate constant does not depend on pH, and the same final product is formed in the entire neutral – alkaline pH range. The only exception is *N*-chloro sarcosine which decomposes via two parallel reaction paths – one pH-independent and one first-order for the hydroxide ion – leading to different end products. At physiological pH, the decomposition of these compounds results in methylamine and aldehydes, which are not particularly toxic, but may cause taste and odor problems in drinking water treatment technologies.

The time-dependent spectral changes of *N*-chloro-*N*-methylalanine (NCMA), *N*-chloro-*N*-methylleucine (NCML), *N*-chloro-*N*-methylisoleucine (NCMI) and *N*-chloro-*N*-methylvaline (NCMV) show very similar kinetic behavior in the entire neutral-alkaline pH range (Figure 8).

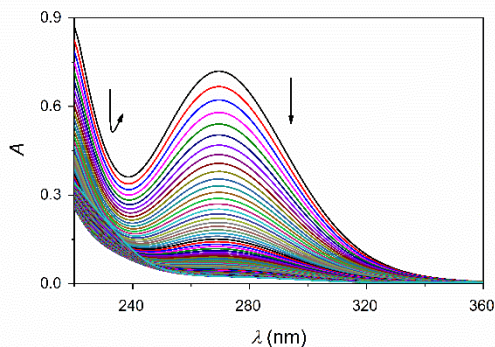


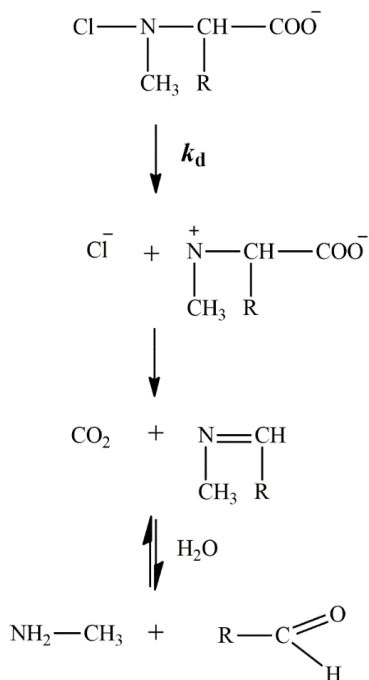
Figure 8. Time-resolved spectral changes during the decomposition of NCMA under alkaline conditions.

$c_{\text{NCMA}}^0 = 3.00 \times 10^{-3} \text{ M}$, $c_{\text{NMA}}^0 = 3.00 \times 10^{-3} \text{ M}$, $c_{\text{OH}^-} = 5.00 \times 10^{-2} \text{ M}$, $I = 1.00 \text{ M (NaClO}_4)$, $T = 25.0 \text{ }^\circ\text{C}$, $\Delta t = 5 \text{ s}$, $t = 1000 \text{ s}$.

We have demonstrated that the rate coefficients of these first-order reactions are independent of pH in the 6.0 – 13.0 region. The rate coefficient decreases as the size of the alkyl side chain on the α -carbon increases, indicating the importance of steric effects.

^1H NMR experiments were carried out to identify intermediates and products as well as to monitor their concentration profiles. The NMR results for the NCMA, NCML, NCMI and NCMV systems are completely analogous. We have proven that methylamine and the corresponding aldehyde are the final products in neutral medium, while a Schiff base is formed in an equilibrium reaction of these two products under alkaline conditions.

We have developed a detailed mechanism for the decomposition reactions of *N*-chloro-*N*-methyl alkyl-substituted amino acids (Scheme 1).



Scheme 1. Common kinetic model for the decomposition of NCMG (only under neutral conditions), NCMA, NCML, NCMI and NCMV.

We have shown that the products of the decomposition of *N*-chloro-*N*-methyl glycine in an alkaline medium are methylamine and glyoxalate ion.

4. We have confirmed that *N,N*-dichloroamino acids are not formed in the reactions of glycine, α -alanine, and branched chain amino acids (leucine, isoleucine, valine) with excess hypochlorous acid under alkaline conditions. In all cases, the fast formation of *N*-monochloroamino acid, its decomposition in a rate-determining step, and further oxidation of the intermediate products take place. We identified the products using ^1H NMR method and established that they form according to first-order kinetics. We have developed detailed mechanisms for these processes.

Under alkaline conditions, the oxidation of glycine (gly), α -alanine (ala), leucine (leu), isoleucine (ileu) and valine (val) by excess hypochlorous acid yields the corresponding *N*-monochloroamino acids. We have proven that the reactions are first-order for both amino acids and HOCl, and the second-order rate constants are in good agreement with earlier results.

During the significantly slower second part of the reaction, the absorbance at the characteristic absorption band of OCl^- ($\lambda_{\text{max}} = 292 \text{ nm}$) decreases significantly according to first-order kinetics. We have confirmed that the rate constant of this process is independent of the concentration of HOCl and corresponds to the rate-determining decomposition of *N*-monochloro amino acids. Based on the ^1H NMR spectra, we have identified the products of the reactions (Figure 9) and studied their formation kinetics. The rate constants obtained from spectrophotometric and NMR measurements are the same within the margin of error, i.e. the time profiles of the processes are determined by the same rate-determining step.

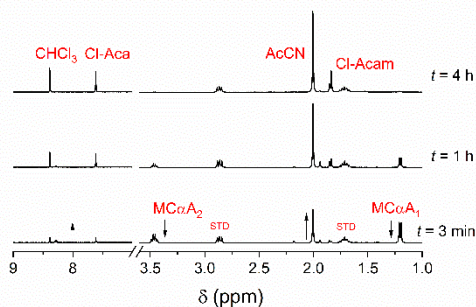


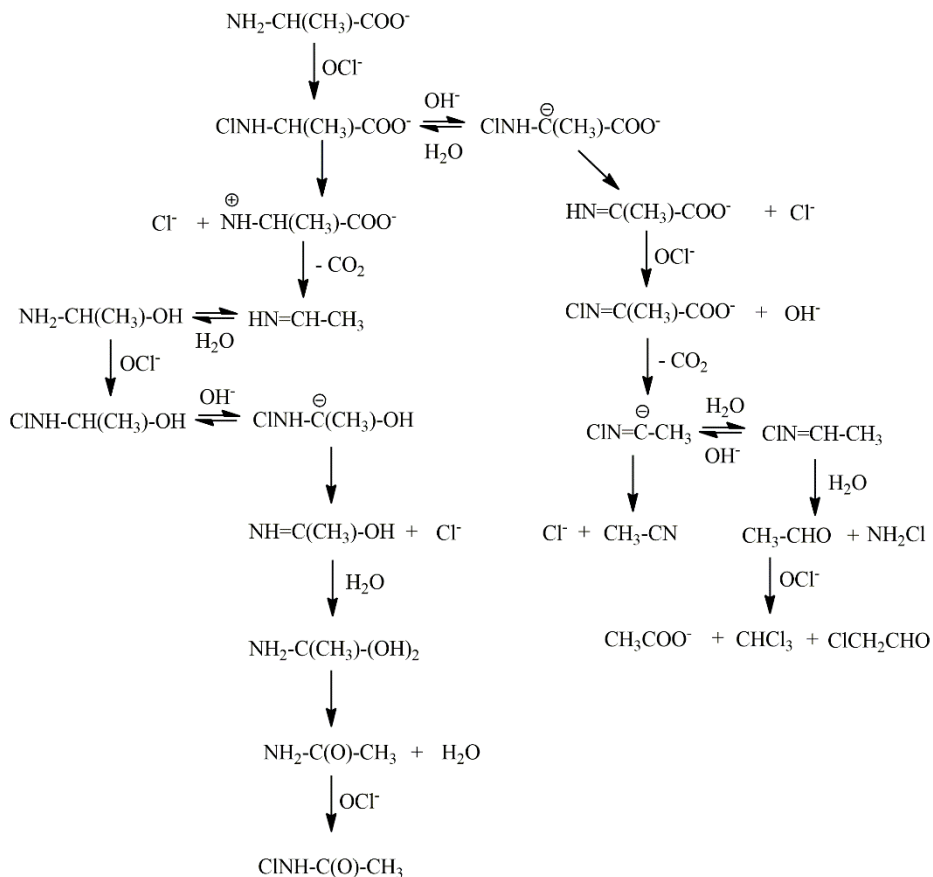
Figure 9. Time-dependent ^1H NMR spectra during the decomposition reaction of $\text{MC}\alpha\text{A}$ under alkaline conditions. The arrows indicate the changes of intensities. Peak assignments: $\text{MC}\alpha\text{A}$: *N*-chloro- α -alanine, Cl-Acam : chloro acetamide, AcCN : acetonitrile, CHCl_3 : chloroform, Cl-Aca : chloro acetaldehyde, STD : standard.

$c_{\text{ala}}^0 = 7.50 \times 10^{-3} \text{ M}$, $c_{\text{HOCl}}^0 = 3.75 \times 10^{-2}$, $c_{\text{OH}^-} = 5.00 \times 10^{-2} \text{ M}$,
 $T = 25.0 \text{ }^\circ\text{C}$.

We have proposed detailed mechanisms in accordance with the experimental results. In the case of *N*-chloro- α -alanine ($\text{MC}\alpha\text{A}$), a carbanion is formed from the *N*-monochloroamino acid in a fast acid-base pre-equilibrium, and the primary decomposition takes place via two reaction pathways (Scheme 2). After that, the products are formed through rapid hydration, hydrolytic and chlorination steps.

We have proven that the mechanism is simplified by increasing the α -alkyl side chain. In the case of branched chain amino acids, the decomposition takes place only through the carbanion and the corresponding nitrile, chloroacetaldehyde and other chlorinated derivatives are formed as end products.

We found that the decomposition of *N*-chloroglycine also takes place exclusively through the carbanion path. In this case formamide and cyanate ion are formed as end products.



Scheme 2. The mechanism of the chlorination of α -alanine under alkaline conditions.

5. We have shown that during the chlorination of glycine, α -alanine and branched-chain amino acids (leucine, isoleucine, valine) with excess hypochlorous acid under neutral conditions, the corresponding *N*-monochloro amino acids form extremely quickly. In the next step, they are oxidized to *N,N*-dichloroamino acids by dichloro monoxide (Cl_2O). The dichloro derivatives undergo decarboxylation in a few seconds yielding the corresponding *N*-chloroimines. These intermediates are transformed in slow decomposition reactions. The intermediate and final products were identified using a time-dependent ^1H NMR method and detailed mechanisms were established for these reactions.

The kinetic curves of the reactions of α -alanine and branched-chain amino acids with an excess of hypochlorous acid recorded with the *stopped-flow* method show two, partially overlapping, first-order processes after a rapid jump in absorbance (Figure 10). The first-order processes are assigned to the oxidation of monochloroamino acid to dichloroamino acid ($k_{\text{obs}1}$) and the transformation of the dichloro derivative into a relatively stable intermediate ($k_{\text{obs}2}$).

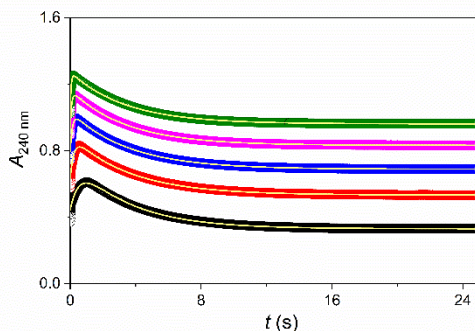


Figure 10. Typical experimental (markers) and fitted (continuous lines) kinetic traces for the formation and conversion of DC α A at different concentrations of HOCl under neutral condition. The traces were fitted to the sum of two exponential equation.

$c_{\text{ala}}^0 = 5.00 \times 10^{-4} \text{ M}$, $c_{\text{HOCl}}^0 = \bullet 5.50 \times 10^{-3} \text{ M}$, $\bullet 8.00 \times 10^{-3} \text{ M}$,
 $\bullet 1.05 \times 10^{-2} \text{ M}$, $\bullet 1.30 \times 10^{-2} \text{ M}$, $\bullet 1.55 \times 10^{-2} \text{ M}$, $\text{pH} = 6.74$,
 $I = 1.0 \text{ M (NaClO}_4\text{)}$, $T = 25.0 \text{ }^\circ\text{C}$.

The plot of $k_{\text{obs}1}/c_{\text{HOCl,corr}}$ as a function of $c_{\text{HOCl,corr}}$ is a straight line with zero intercept, where $c_{\text{HOCl,corr}}$ is the concentration of HOCl corrected with the amount consumed by the formation of *N*-chloroamino acids (Figure 11). Accordingly, the formation of *N,N*-dichloroamino acids are second order reactions with respect to hypochlorous acid, and overall third-order processes. These results confirm that Cl_2O is the reactive form in the chlorination. We have confirmed that $k_{\text{obs}2}$ is independent of HOCl concentration.

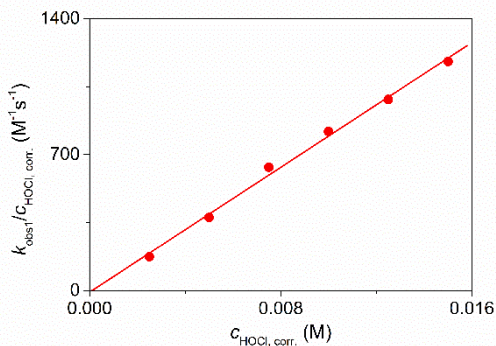
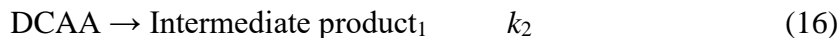


Figure 11. The dependence of k_{obs1} on the concentration of HOCl under neutral conditions in the Ala – HOCl system.

$c_{\text{ala}}^0 = 5.00 \times 10^{-4} \text{ M}$, $\text{pH} = 6.74$, $I = 1.0 \text{ M}$ (NaClO_4), $T = 25.0 \text{ }^\circ\text{C}$.

We have proposed a kinetic model that provides excellent interpretation of the experimental results (equations (13) – (16)).



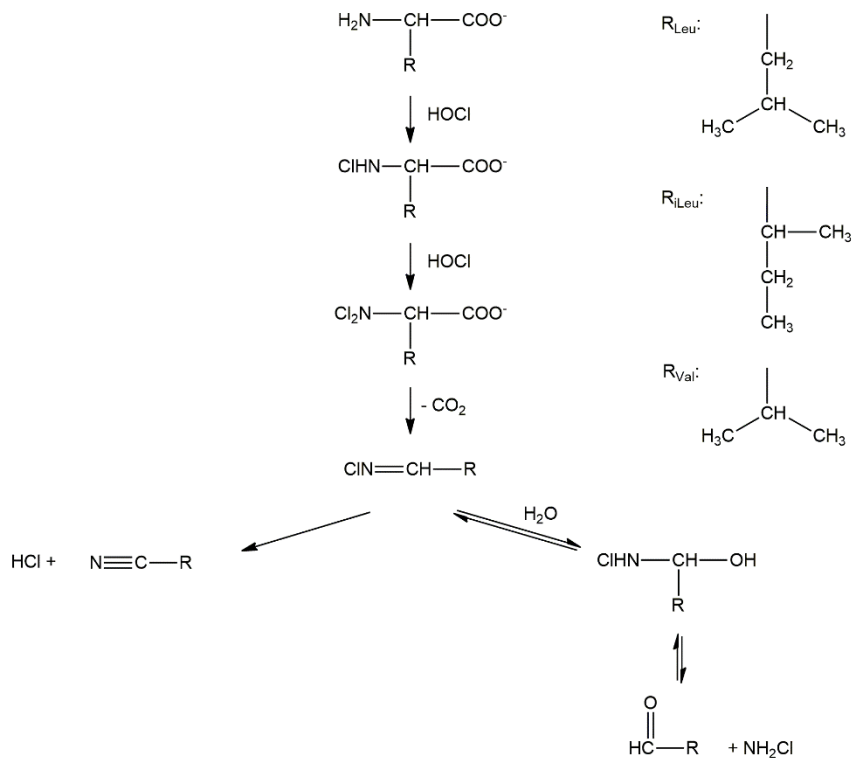
In the case of glycine, the dichloro derivative is transformed in several overlapping processes and the fitting of the kinetic traces with acceptable reliability is not feasible.

Table 3. The kinetic parameters, k_{Cl_2O} K_1 and k_2 , for the formation and decomposition of the *N,N*-dichloroamino acids.

$T = 25.0$ °C.

Amino acid	$k_{Cl_2O} K_1 \times 10^4$ ($M^{-1}s^{-1}$)	k_2 (s^{-1})	pH
α -alanine	8.0 ± 0.3	0.29 ± 0.01	6.74
leucine	6.9 ± 0.4	0.70 ± 0.02	6.92
isoleucine	6.2 ± 0.2	0.58 ± 0.03	6.92
valine	7.3 ± 0.4	0.46 ± 0.01	6.92
glycine	8.7 ± 0.3	-	6.91

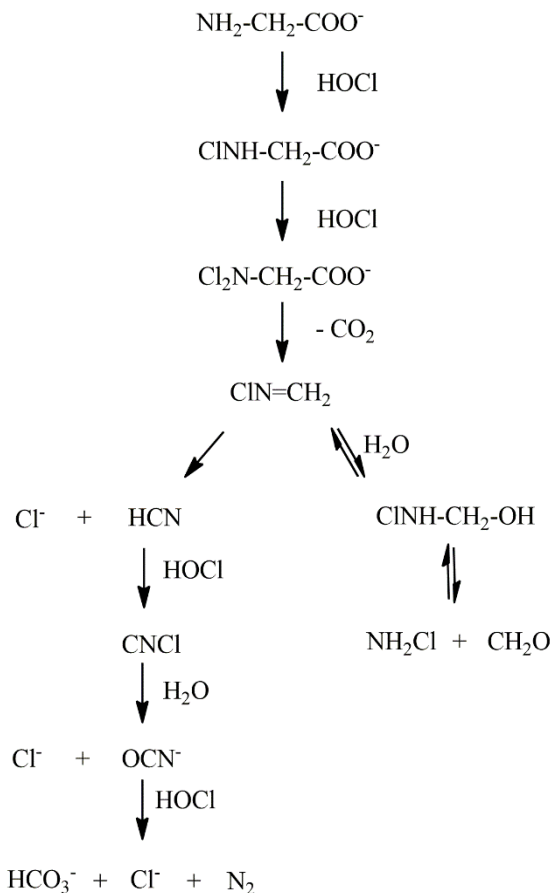
Based on 1H NMR spectra, we confirmed that *N*-chlorimine is formed as an intermediate product in reaction (16), the transformation of which was followed by the time-dependent NMR method. We have confirmed that a nitrile derivative is formed as a final product in the case of branched-chain amino acids, which is also detected in alkaline media (Scheme 3).



Scheme 3. The mechanism of the chlorination of leucine, isoleucine and valine under neutral conditions.

In the case of α -alanine the acetaldehyde is further oxidized to acetic acid.

In the case of glycine, the initial transformation of the dichloro derivative is consistent with the general mechanism, however, HCN is further oxidized and complete mineralization takes place through the formation of OCN^- (Scheme 4). The change in the concentration of this latter intermediate was monitored using ion chromatography.



Scheme 4. The mechanism of the chlorination of glycine under neutral conditions.

Possible utilization of the results

We have extensively studied the kinetics and mechanism of the chlorination processes between hypochlorous acid and ammonia, *N*-methylamino acids, and five different amino acids. The formation and decomposition kinetics of chloramines, *N*-chloro-*N*-methylamino acids, and *N*-chloro- and *N,N*-dichloroamino acids have been described in detail.

We have identified the intermediates and final products, as well as their relative amounts. This may contribute to the identification of various compounds formed in water purification processes and to the assessment of their impact on water quality. These compounds are of utmost importance in the toxicological quality of the produced drinking water, as well as they may cause unwanted odor and taste problems. Our results can contribute to the optimization of water purification technologies, thus to the production of better quality drinking water.

Among the investigated processes, some of the reactions also have an important role in biological systems. Establishing the detailed mechanism of the investigated processes is also important in the interpretation of *in vivo* processes.



Registry number: DEENK/50/2023.PL
Subject: PhD Publication List

Candidate: Fruzsin Simon
Doctoral School: Doctoral School of Chemistry
MTMT ID: 10064784

List of publications related to the dissertation

Foreign language scientific articles in international journals (2)

1. **Simon, F.**, Szabó, M., Fábíán, I.: The chlorination of glycine and alpha-alanine at excess HOCl: Kinetics and mechanism.
J. Hazard. Mater. 447, 1-9, 2023. ISSN: 0304-3894.
DOI: <http://dx.doi.org/10.1016/j.jhazmat.2023.130794>
IF: 14.224 (2021)
2. **Simon, F.**, Kiss, E., Szabó, M., Fábíán, I.: The chlorination of N-methyl amino acids with hypochlorous acid: kinetics and mechanisms.
Chem. Res. Toxicol. 33 (8), 2189-2196, 2020. ISSN: 0893-228X.
DOI: <http://dx.doi.org/10.1021/acs.chemrestox.0c00222>
IF: 3.739

List of other publications

Foreign language scientific articles in international journals (3)

3. Szabó, M., Bíró, V., **Simon, F.**, Fábíán, I.: The decomposition of N-chloro amino acids of essential branched-chain amino acids: kinetics and mechanism.
J. Hazard. Mater. 382, 1-8, 2020. ISSN: 0304-3894.
DOI: <http://dx.doi.org/10.1016/j.jhazmat.2019.120988>
IF: 10.588
4. **Simon, F.**, Szabó, M., Fábíán, I.: pH controlled byproduct formation in aqueous decomposition of N-chloro- α -alanine.
J. Hazard. Mater. 362, 286-293, 2019. ISSN: 0304-3894.
DOI: <http://dx.doi.org/10.1016/j.jhazmat.2018.09.004>
IF: 9.038





**UNIVERSITY of
DEBRECEN**

**UNIVERSITY AND NATIONAL LIBRARY
UNIVERSITY OF DEBRECEN**

H-4002 Egyetem tér 1, Debrecen
Phone: +3652/410-443, email: publikaciok@lib.unideb.hu

5. Szabó, M., **Simon, F.**, Fábíán, I.: The formation of N-chloramines with proteinogenic amino acids.
Water Res. 165, 1-8, 2019. ISSN: 0043-1354.
DOI: <http://dx.doi.org/10.1016/j.watres.2019.114994>
IF: 9.13

Total IF of journals (all publications): 46,719

Total IF of journals (publications related to the dissertation): 17,963

The Candidate's publication data submitted to the iDEa Tudóstér have been validated by DEENK on the basis of the Journal Citation Report (Impact Factor) database.

22 February, 2023

